VNU Journal of Science: Natural Sciences and Technology
Journal homepage: https://js.vnu.edu.vn/NST

Original Article

Adhesion and Cathodic Delamination Properties of Epoxy Coating Reinforced by Magnetite/Hydroxyapatite on Carbon Steel Substrate

Thai Thu Thuy[1,*], Tran Tien Dat[2], Nguyen Thi Thu Uyen[2], Luong Hoang Minh[2], Nguyen Xuan Hoan[2], Trinh Anh Truc[1]

[1]*Institute for Tropical Technology, Vietnam Academy of Science and Technology, 18 Hoang Quoc Viet, Cau Giay, Hanoi, Vietnam*

[2]*VNU University of Science, Faculty of Chemistry, 19 Le Thanh Tong, Hoan Kiem, Hanoi, Vietnam*

Received 10th November 2023
Revised 10th December 2024; Accepted 18th December 2024

Abstract: In this study, magnetite/hydroxyapatite nanoparticles were incorporated at a concentration of 5 wt.% to enhance both the adhesion strength and cathodic delamination resistance of an epoxy coating applied to a carbon steel substrate. Magnetite/hydroxyapatite (FoHAP) was prepared with varying Fe_3O_4 to hydroxyapatite weight ratios, ranging from 10 to 50 wt.%. The adhesion test was quantitatively assessed using the pull-off method following the ASTM D4541 standard and qualitative evaluations were conducted using the cross-cut method following the ASTM D3359 standard. The results demonstrated that the coating reinforced with magnetite/hydroxyapatite nanoparticles exhibited a superior adherence compared to both the unpigmented epoxy and the coating with hydroxyapatite alone. Furthermore, assessments of the cathodic delamination process and the electrochemical impedance spectroscopy revealed that the optimized Fe_3O_4/HAP ratio of 10 wt.% correlated with a reduced area of delamination, indicating the reinforcement in cathodic delamination protection and also the adhesion properties of the nanoparticle-enhanced coating.

Keywords: Magnetite/hydroxyapatite, adhesion, cathodic delamination, EIS, corrosion.

1. Introduction

In recent years, nanosized pigments such as SiO_2, CeO_2, Co_3O_4, and TiO_2 in paint formulation helped to increase the anticorrosion properties, also thermal and mechanical properties of nanocomposite-based coatings [1-4]. There were also numerous reports about the addition of Fe_3O_4 nanoparticles in organic coatings thanks to their inhibitive and non-poisonous effects. However, due to their significant surface energy, Fe_3O_4 nanoparticles tend to agglomerate easily. This phenomenon can lead to some interfacial and surficial defects

* Corresponding author.
E-mail address: ttthuy@itt.vast.vn

https://doi.org/10.25073/2588-1140/vnunst.5623

during coating application - resulting in the reduction of coating properties. So to limit this fact, Fe_3O_4 nanoparticles need a surface modification or to produce magnetite-based nanocomposite [2, 5-7].

A previous study has reported the modification of magnetite nanoparticles with indole-3-butyric acid (IBA) as a pigment in epoxy-polyamide paint formulation [5]. The coating contained Fe_3O_4 and IBA-treated Fe_3O_4 showed the reinforcement in anticorrosion protection and adherence performance with carbon steel substrate. This strength in barrier properties and adhesion behavior and links to the good dispersion of magnetite particles in the epoxy-polyamide matrix due to the IBA organic part. IBA-treated Fe_3O_4 particles become more compatible with the polymer matrix, resulting in a complete polymer network. The improvement in anticorrosion protection is also thanks to the release of IBA particles (as anodic inhibitor) in an alkaline medium that prevents the corrosion process.

Cobalt-doped magnetite nanoparticles ($CoFe_2O_4$) were synthesized via the hydrothermal method [3]. The reinforcement in barrier properties of the epoxy coating for carbon steel was achieved with the low doped concentration of $CoFe_2O_4$ (3 wt.%). The improvement of cobalt-doped magnetite nanoparticles in the corrosion protection of $CeFe_2O_4$-contained water-based epoxy coating was also approved for the 2024 aluminum alloy substrate [8]. Although the cobalt content modified the synthesized magnetite nanoparticles was low (2.5 wt.% of cobalt), the barrier properties of epoxy coating covered on 2024 aluminum alloy were maintained until 49 days of immersion in a corrosive environment. This is related to the inhibitive effect of magnetite nanoparticles and also to the formation of cobalt hydroxide at cathodic sites.

Recently, Asif et al. described the use of HAP/Fe_3O_4 nanocomposite which was prepared via the co-precipitation method as filler in polyurethane matrix [9]. The mechanical properties of HAP/Fe_3O_4-contained polyurethane coating were reported but the role of HAP/Fe_3O_4 had not been mentioned.

In this study, magnetite/hydroxyapatite (FoHAP) is prepared and incorporated into an epoxy matrix at 5 wt.%. The FoHAP composite was prepared from Fe_3O_4 (Fo) and hydroxyapatite (HAP) nanopowders (obtained via hydrothermal synthesis), according to the ratio of Fe_3O_4/HAP varied from 10 to 50 wt.%. The adhesion measurements combine with the cathodic accelerated test that will be used to evaluate and prove the role of magnetite/hydroxyapatite in the epoxy coating films to prevent the corrosion of carbon steel.

2. Material and Experimental Techniques

2.1. Materials

The carbon steel CT3 substrates (10×15×0.1) cm were firstly cleaned with an alkaline solution to remove oil excess on their surface; then treated with grinding paper followed by 100, 400, and 1200 grit before applying the epoxy coating layer.

Hydroxyapatite and magnetite nanoparticles were separately synthesized followed by the hydrothermal method [10]. As-prepared hydroxyapatite particles were magnetically dispersed in the mixture of distilled water/ethanol absolute (8/2 vol./vol.) for 30 min. Magnetite nanoparticles were then slowly inserted in this mixture followed by the ratio of Fe_3O_4/HAP: 1/10 (10FoHAP), 1/5 (20FoHAP), and 1/2 (50FoHAP) in weight, respectively. The FoHAP mixture was then refluxed at 80 ^oC for 6 hours. Finally, the products were collected by centrifugation and dried at 80 ^oC for 24 hours.

5 wt.% of FoHAP mixture, as a filler, incorporated in the epoxy coatings were prepared by spin-coating technique with the use of Epoxy YD828 and Hardener Epicure 8537. The reference specimens without filler and the

5 wt.% HAP-contained epoxy coating (HAP/EP) was also prepared. The film thickness was about 30 ± 3 µm.

2.2. Experimental Techniques

Surface charges of Fe_3O_4, HAP, and FoHAP particles were analyzed at room temperature under the applied voltage of 100 Volts by using Zeta Phoremeter IV (CAD Instrumentation). The sample was dispersed and sonicated in the 10^{-3} M KCl solution. The sample was measured and repeated at least 15 times to get the average values of Zeta potential by using the Smoluchowski approximation.

Scanning electron microscopy was employed to characterize the morphology of FoHAP particles with the aid of Hitachi S-4800.

The adhesion behaviour of FoHAP incorporated in an epoxy coating on carbon steel CT3 substrate was examined by a pull-off test (following ASTM D4541 standard) and an Elcometer 1542 cross-hatch adhesion test (followed by ASTM D3359 standard). A digital microscope Keyence VH-Z100 was used to observe the surface of the epoxy coating films and the surface of the CT3 substrate.

A cathodic delamination test was carried out on the painted substrate (after creating a standard scratch 20 mm in length on the surface) with the help of a Biologic VSP-300 potentiostat in 0.1 M Na_2SO_4 solution. 5 cycles of accelerated tests were continuously applied out of which one included 60 min. at -1.2 V vs Ag/AgCl/ saturated KCl reference electrode then 60 min. at open circuit potential. After each test cyclic procedure, the electrochemical impedance spectroscopy (EIS) was conducted on the sample in the appropriate condition: the frequency range from 10 kHz to 10 mHz, 6 points per decade with 10 mV of amplitude. The surface and appearance change of the coating layers after the end of EIS characterization was also observed and analyzed by a Keyence VH-Z100 3D digital microscope.

3. Results and Discussion

3.1. Characterization of FoHAP Nanopowders

Figure 1 represents the morphology of 10FoHAP nanopowders as a representative detected by FE-SEM. The hydroxyapatite (HAP) nanoparticles were known as a rod-like crystalline structure [10]. In the case of the magnetite nanoparticles, the morphology presented as a uniform spherical shape with a grain size in the range of 30 - 40 nm. The Fo nanoparticles were well attached with the HAP particles.

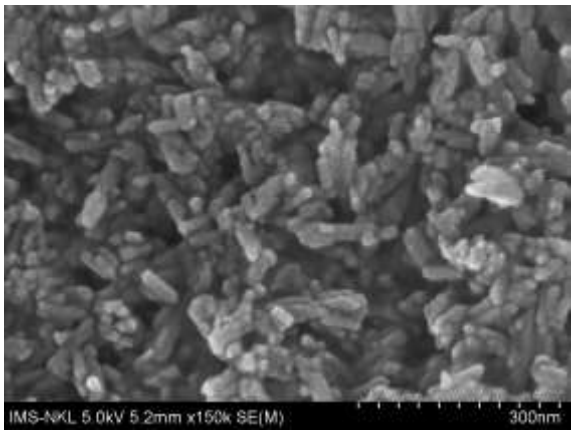

Figure 1. FE-SEM observation of 10FoHAP.

Table 1 reported the results of the Zeta potential of Fe_3O_4 (Fo), Hydroxyapatite (HAP), and FoHAP composites.

Table 1. Results on Zeta potential of Fe_3O_4, HAP, and FoHAP nanoparticles

Sample	Zeta potential (mV)
Fe_3O_4	-29.19
HAP	-25.29
10FoHAP	-25.59
20FoHAP	-26.89
50FoHAP	-27.41

The average surface charge values of FoHAP composite are in the range of -29.2 mV (Fe_3O_4) and -25.3 mV (HAP) respectively. Herein,

the negative charge on the surface of particles is a result of the adsorption/attachment of hydroxyl groups (-OH) from the alkaline medium of hydrothermal reaction [10]. A slight increment in the value of the surface charge on the FoHAP composite sample is compatible and in agreement with the ratio of Fe_3O_4/HAP in samples.

3.2. Effects of FoHAP on the Adhesion Performance of Epoxy-Based Organic Coating

Fracture surface observation of epoxy coating containing 5 wt.% of 10FoHAP was characterized by FE-SEM and presented in Figure 2. As can be observed, the FoHAP composites were well dispersed in the epoxy matrix, followed by a relatively smooth epoxy structure. Some accumulations were also detected but it was difficult to report the interfacial boundary between the epoxy and the filler. This resulted in the compatibility of the doped-FoHAP with the epoxy network, and also a reinforcement in the internal adhesion.

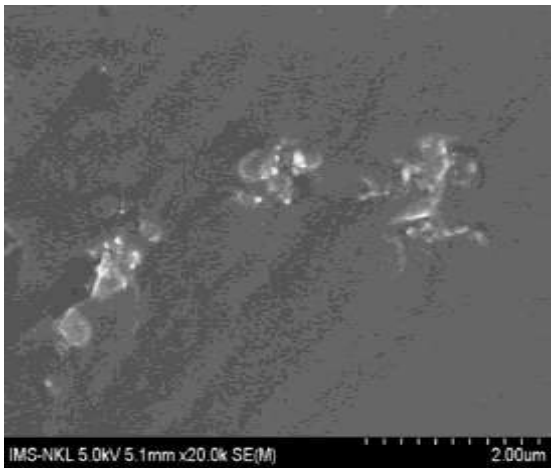

Figure 2. Cross-section image by FE-SEM of epoxy coating containing 5 wt.% 10FoHAP.

Table 2 presents the results according to the adhesion test followed by ASTM D4541 and ASTM D3359 standards. The surface appearance of the sample after applying the adhesion test following the ASTM D3359 standard was reported in Figure 3.

Table 2. Adhesion results of painted epoxy systems

Sample	Pull-off test (MPa)	Cross-cut test
Epoxy (EP)	1.43 ± 0.28	3B
HAP/EP	1.38 ± 0.91	3B
10FoHAP/EP	2.37 ± 0.47	4B
20FoHAP/EP	2.20 ± 0.34	4B
50FoHAP/EP	1.09 ± 0.29	3B

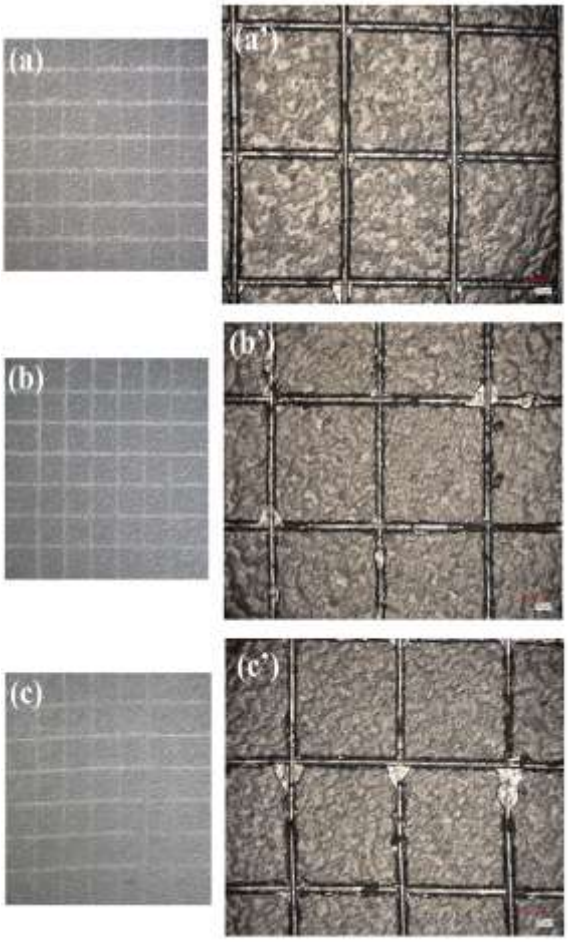

Figure 3. Surface appearance of 10FoHAP/EP (a, a'), 20FoHAP/EP (b, b'), 50FoHAP/EP (c, c') after adhesion test followed ASTM D3359 standard.

As can be seen, incorporating pigments into paint formulation can bring a change in the

adhesion behavior. From the results of the pull-off test, the epoxy-containing HAP got a slight decrease (1.38 MPa) in the adhesion value compared to the one obtained for the epoxy sample (1.43 MPa). Thus the hydroxyapatite particles did not enhance the adhesion strength. On the other hand, the presence of magnetite/hydroxyapatite raised this behavior depending on the percentage of magnetite amounts. The epoxy-containing 10FoHAP and 20 FoHAP nanopowders showed a higher value compared to the film containing 50FoHAP. This trend was accepted by the results acquired from the cross-hatch adhesion test. Based on the ASTM D3359 standard, the surface area loss after cross-hatch adhesion test corresponded to the 10FoHAP and 20FoHAP-based epoxy varied from 5-15% in comparison to the tested surface at the beginning; while in the case of 50FoHAP, the peeled off area was approximately about 15-25%. The removed surface area after the cross-hatch adhesion test can be observed clearly in Figure 3. In Figure 3a, a', the removed organic coating was concentrated only in the cut-through the coating down to the substrate, indicating the good adhesion of 10FoHAP-based epoxy film. In the case of 20FoHAP-based coating, Figure 3b, b' respectively, the film removal was not only localized to the cut but also to observe a small part of the surrounding area, the total peeled-off area was less than 15% (4B classification identification). Adding a higher amount of magnetite particles on the hydroxyapatite surface (50 wt.%) didn't improve the adhesion between the epoxy coating layer and the CT3 substrate, Figure 3c, c'.

3.3. Effects of FoHAP on the Cathodic Delamination of Epoxy Based Organic Coating

Figure 4 shows the surface appearance of samples after 5 cycles of cathodic delamination measurement. The extent of the scratch after the test was analyzed and reported in Table 3.

Table 3. Parameters corresponded to the extended detachment

Samples	Width of scratch (µm)	Rugosity (µm)
Epoxy (EP)	313 - 324	64.63
HAP/EP	239 - 366	61.56
10FoHAP/EP	73 - 81	49.89
20FoHAP/EP	60 - 66	43.41
50FoHAP/EP	57 - 69	55.27

Firstly, the red rust was visually observed at the scratch as seen in Figure 4a, it is related to the corrosion phenomenon that occurred on the reference (epoxy coating) sample. This result was similarly observed when examined the hydroxyapatite-contained epoxy coating, Figure 4b respectively. In this case, the detachment was extended along the scratch up to 366 µm and the corrosion was not kept in line compared to the image obtained for the reference sample, Figure 4a'. Due to the potential applied during the cathodic delamination process, the epoxy was peeled off from the substrate following the visible permeation of water throughout the defect (dashed line marked in Figure 4a,b). The roughness when removing HAP-based epoxy coating was measured at approximately 61.6 µm (as seen in Figure 4b''), comparable with 64.6 µm (Figure 4a'') in roughness detected in the reference sample. The added hydroxyapatite particles did not improve the protection of the epoxy coating as well as the neat epoxy (reference sample).

This delamination was limited by the presence of magnetite/hydroxyapatite nanoparticles in the coating formulation, Figure 4c, d, e respectively. As can be seen, both the elimination of epoxy film and the width of the scratch were reduced, in the range of 60 – 80 µm, lower than 4 times when compared to the value

obtained for the reference sample (313-324 µm). The cathodic delamination process caused the adhesion loss due to the generation of hydroxyl ions at the coating/metal interface, resulting in the increment of removal epoxy layer [11, 12]. Regarding the results in Figure 4, the different behavior between the reference sample, the HAP-based epoxy coating, and the FoHAP-based epoxy film can be attributed to the retardment corrosion activity of magnetite particles. These nanoparticles can consume the OH^- ions generated from the cathodic process by creating hydrogen bonds, limiting the adhesive delamination.

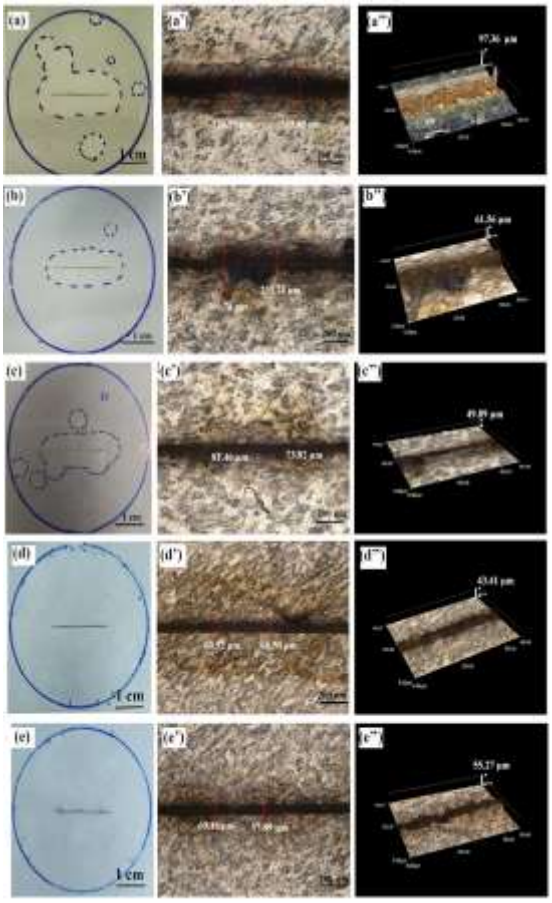

Figure 4. The surface appearance of epoxy coating as reference (a, a', a") and HAP/EP (b, b', b''), 10FoHAP/EP (c, c', c''), 20FoHAP/EP (d, d', d''), 50FoHAP/EP (e, e', e'') after 5 cyclic cathodic delamination process.

However, the increment of doped magnetite particles is not logically linked to the protective effect. The delaminated epoxy film in the case of 50FoHAP-based coating (Figure 4 e") was more noticeable than in the case of coating containing 10FoHAP and 20FoHAP. In combination with the result of the adhesion test, the large amount of doped-magnetite in hydroxyapatite (50FoHAP) does not support the adhesion strength in the delaminated area. By contrast, the 10FoHAP and 20FoHAP-based epoxy coating presented good protection in adhesion and cathodic protection properties with carbon steel substrate.

Electrochemical impedance spectroscopy (EIS) can be used to characterize the adhesion behavior of organic coating. In this study, the EIS diagrams were measured before the first cyclic cathodic procedure (T0) and after each time the cyclic finished (T1, T2, T3, T4, T5). Figure 5 presents the Bode modulus and phase diagram obtained for the 50FoHAP-based coating following the cathodic process, as an example. A fast degradation of barrier properties can be observed after the first applied potential (T1) compared to the initial state (T0). The modulus value at low frequency decreased about 10 times in magnitude and then continuously reduced till the end of the measurement.

In this case, the double-layer capacitance C_{dl} was a factor depending on the development of the delaminated area [14]. Besides that, applying a cathodic potential of -1.2 V (vs the reference electrode) led to an electrochemical degradation of organic coating resistance which strongly affected the scratch. As a consequence, the increase of C_{dl} after each cycle of cathodic delamination related to the extent of the artificial scratch at the carbon steel substrate [13, 14].

To characterize in deepness the reinforcement of magnetite/hydroxyapatite in the adhesion of the epoxy coating, the double-layer capacitance was extracted from the experimental impedance spectroscopy data with an equivalent circuit model.

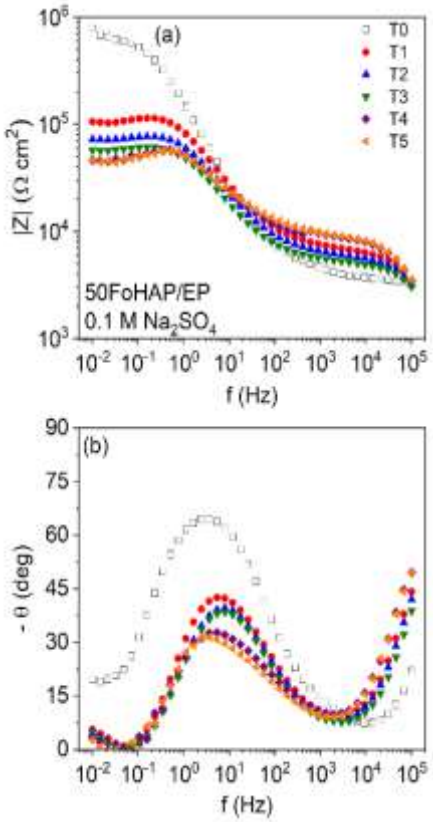

Figure 5. Bode modulus (a) and phase (b) diagrams of 50FoHAP-based epoxy coating before each cyclic cathodic delamination test.

Figure 6 represented the equivalent electrical circuit used for interpreting experimental data (a): C_p is the organic coating capacitance and R_p is the resistance of the electrolyte solution in the defect, while C_{dl} and R_{dl} are the double layer capacitance and charge transfer resistance corresponded to the interface coating/metallic substrate [13].

After fitting with the help of ZSimpWin 3.5 modeling software, the evolution of C_{dl} followed the number of cyclic delamination processes obtained for the 50FoHAP-based coating is shown in Figure 6 b.

To highlight the difference in adhesion reinforcement between the pigment-based coating, the value of the double layer capacitance obtained after the fifth cyclic (T5) was divided by the one of the initial C_{dl} (T0) to obtain the ratio of delaminated area, Figure 7 respectively. This ratio can be attributed to the degree of detachment of the coating from the substrate: the higher the parameter, the more the adhesion loss.

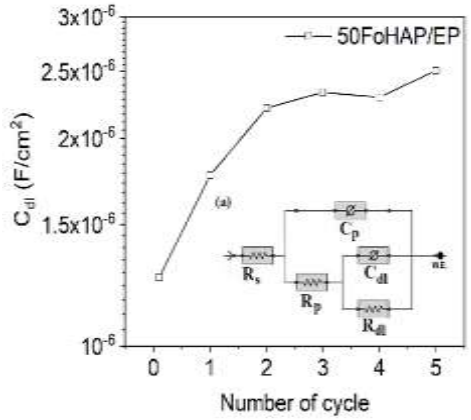

Figure 6. Electrical equivalent circuit used for interpreting experimental data (a) and evolution of double-layer capacitance obtained for 50FoHAP-based epoxy coating (b).

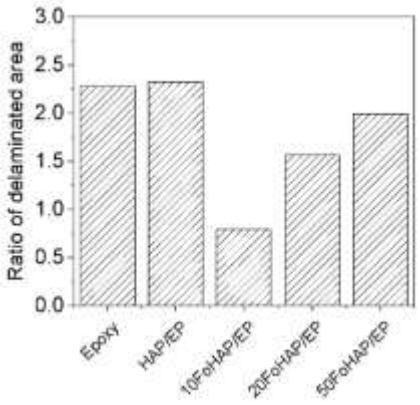

Figure 7. Ratio of delaminated area (final C_{dl}/initial C_{dl}) of all experimental coating systems.

Regarding the ratio of delamination in Figure 7, the value obtained for the 10FoHAP-based coating showed a notably lower result when compared with the 20FoHAP and the 50FoHAP. The unpigmented epoxy and the HAP-based epoxy coating showed a high ratio. This fact was approved by the effect of 10FoHAP in the reinforcement of adhesion of epoxy-based organic coating with the carbon steel substrate, mainly in the cathodic delamination protection.

4. Conclusion

This work reported the reinforcement effect of magnetite/hydroxyapatite (FoHAP) on the adhesion performance of the epoxy-based organic coating. Magnetite and hydroxyapatite nanoparticles were synthesized via a hydrothermal process with the ratio of Fe_3O_4/hydroxyapatite varied from 10 to 50 wt.%. Subsequently, 5 wt.% of FoHAP particles were then added to the epoxy coating as pigmented powder. The adhesion measurements and the cathodic delamination process proved the effect of FoHAP, especially the 10FoHAP in the reduction of adhesion loss while the presence of HAP alone did not contribute to an enhancement of film adherence. Concerning the reinforcement of 10FoHAP in the adhesion behavior of nanoparticle-based epoxy coating, the delaminated area in cathodic delamination was limited, resulting in the strengthening of anticorrosion properties of 10FoHAP-contained organic coating in a corrosive medium.

Acknowledgements

The authors would like to thank ITT-VAST for financial support.

References

[1] A. C. Balaskas, I. A. Kartsonakis, L. A. Tziveleka, G. C. Kordas, Improvement of Anti-Corrosive Properties of Epoxy-Coated AA2024-T3 with TiO_2 Nanocontainers Loaded with 8-hydroxyquinoline, *Progress in Organic Coatings*, Vol. 74 , 2012, pp. 418-426, https://doi.org/10.1016/j.porgcoat.2012.01.005.

[2] T. T. Thai, A. T. Trinh, G. V. Pham, T. T. T. Pham, H. N. Xuan, Corrosion Protection Properties of Cobalt Salt for Water-Based Epoxy Coatings on 2024-T3 Aluminum Alloy, *Journal of Corrosion Science and Technology*, Vol. 19, No. 1, 2020, pp. 8-15. https://doi.org/10.14773/cst.2020.19.1.8.

[3] T. A. Truc, N. X. Hoan, D. T. Bach, T. T. Thuy, K. Ramadass, C. I. Sathish, N. T. Chinh, N. D. Trinh, T. Hoang, Hydrothermal Synthesis of Cobalt Doped Magnetite Nanoparticles for Corrosion Protection of Epoxy Coated Reinforced Steel, *Journal of Nanoscience and Nanotechnology*, Vol. 20, 2020, pp. 1-8, https://doi.org/10.1166/jnn.2020.17413.

[4] F. Deflorian, M. Fedel, S. Rossi, P. Kamarchik, Evaluation of Mechanically Treated Cerium (IV) Oxides as Corrosion Inhibitors for Galvanized Steel, *Electrochimica Acta*, Vol. 56, 2011, pp. 7833-7844, https://doi.org/10.1016/j.electacta.2011.04.014.

[5] A. T. Trinh, T. T. Nguyen, T. T. Thai, T. X. H. To, X. H. Nguyen, A. S. Nguyen, M. Aufray, N. Pébère, Improvement of Adherence and Anticorrosion Properties of an Epoxy-Polyamide Coating on Steel by Incorporation of an Indole-3 Butyric Acid-modified Nanomagnetite, *Journal of Coatings Technology and Research*, Vol. 13, No. 3, 2016, pp. 489-499, https://doi.org/10.1007/s11998-015-9768-y.

[6] G. Y. Li, Y. R. Jiang, K. L. Huang, P. Ding, J. Chen, Preparation and Properties of Magnetic Fe_3O_4–chitosan Nanoparticles, *Journal of Alloys and Compounds*, Vol. 466, 2008, pp. 451-456, https://doi.org/ 10.1016/j.jallcom.2007.11.100.

[7] N. Yang, S. Zhu, D. Zhang, S. XU, Synthesis and Properties of Magnetic Fe_3O_4-activated Carbon Nanocomposite Particles for Dye Removal, *Materials Letters*, Vol. 62, 2008, pp. 645-647, https://doi.org/10.1016/j.matlet.2007.06.049.

[8] T. T. T. Thuy, T. T. Anh, P. T. T. Tam, N. X. Hoan, Corrosion Protection Properties of Co_3O_4 and $CoFe_2O_4$ Nanoparticles for Water-Based Epoxy Coatings on 2024-T3 Aluminum Alloys, Corrosion Science and Technology, Vol. 22, No. 2, 2023, pp. 90-98, https://doi.org/10.14773/cst.2023.22.2.90.

[9] A. H. Asif, M. S. Mahajan, N. Sreeharsha, V. V. Gite, B. E. A. Dhubiab, B. E. A. Dhubiab, S. H. Nanjappa, G. Meravanige, D. M. Aleyadhy, Enhancement of Anticorrosive Performance of Cardanol Based Polyurethane Coatings by Incorporating Magnetic Hydroxyapatite Nanoparticles, *Materials*, Vol. 15, 2022, pp. 2308, https://doi.org/10.3390/ma15062308.

[10] H. D. Linh, C. P. Anh, C. Viet, L. T. H. Phong, N. X. Hoan, Preparation of the Magnetic Composite Materials Fe_3O_4/Hydroxyapatite and its Application for Removal of 2.4-D and Chrysoidine Crystal, *VNU Journal of Science: Natural Sciences and Technology*, Vol. 37, No. 1, 2021, pp. 35-43, https://doi.org/10.25073/2588-1140/vnunst.5110.

[11] K. N. Allahar, M. E. Orazem, K. Ogle, Mathematical Model for Cathodic Delamination using a Porosity-pH Relationship, *Corrosion Science*, Vol. 49, 2007, pp. 3638-3658, https://doi.org/10.1016/j.corsci.2007.03.024.

[12] M. A. Petrunin, L. B. Maksaeva, N. A. Gladkikh, T. A. Yurasova, M. A. Maleeva, V. E. Ignatenko, Cathodic Delamination of Polymer Coatings from Metals, Mechanism and Preventaion Methods, A Review., *Int. J. Corros. Scale Inhib.*, Vol. 10, No. 1, 2021, https://doi.org/10.17675/2305-6894-2021-10-1-1.

[13] F. Deflorian, L. Fedrizzi, Adhesion Characterization of Protective Organic Coatings by Electrochemical Impedance Spectroscopy, *Journal of Adhesion Science and Technology*, Vol. 13, No. 5, 1999, pp. 629-645, https://doi.org/10.1163/156856199X00154.

[14] M. Fedel, M. G. Olivier, M. Poelman, F. Deflorian, S. Rossi, M. E. Druart, Corrosion Protection Properties of Silane Pre-treated Powder Coated Galvanized Steel, *Progress in Organic Coatings*, Vol. 66, 2009, pp. 118-128, https://doi.org/10.1016/j.porgcoat.2009.06.011.